

# Supplemental Materials

## Interleukin-22 Promotes Proliferation of Liver Stem/Progenitor Cells in Mice and Patients with Chronic HBV Infection

Dechun Feng<sup>1</sup>, Xiaoni Kong<sup>1</sup>, Honglei Weng<sup>2</sup>, Ogyi Park<sup>1</sup>, Hua Wang<sup>1</sup>, Steven Dooley<sup>2</sup>, M. Eric Gershwin<sup>3</sup>, and Bin Gao<sup>1</sup>

### Materials and Methods

*Histological analysis and immunohistochemistry.* Formalin fixed liver samples were processed and paraffin section of 4  $\mu\text{m}$  thickness were stained with hematoxylin and eosin (H&E) for histological analysis. For detection of pSTAT3, paraffin-embedded sections were stained with an anti-pSTAT3 antibody (Cell Signaling Technology, Beverly, MA) after heat-induced epitope retrieval and visualized by DAB. In this paper, we refer to both oval cells in mice and to atypical ductular reactions in patients as LPCs, which can be identified by immunostaining for specific cell surface markers with anti-cytokeratin 19 (CK19) or anti-pan-cytokeratin (pan-CK) antibodies (Dako, Carpinteria, CA).<sup>1,2</sup>

*Immunofluorescence staining.* Heat-induced epitope retrieval and proteinase K pretreatment (20  $\mu\text{g}/\text{ml}$ , for 10 min in room temperature) were employed on liver paraffin sections. For cultured cells, 10% neutral buffered formalin fixation and methanol permeabilization were used before staining. Immunofluorescence double staining was performed by using anti-pan-CK antibody, biotin labeled anti-BrdU antibody (BD Bioscience, San Jose, CA) or anti-pSTAT3 antibody (Cell Signaling Technology). Slides were visualized by Alex488 labeled anti-rabbit antibody (Cell Signaling Technology) and streptavidin labeled Alex555 (Invitrogen, Carlsbad, CA).

*Flow cytometry analyses.* Single cell suspensions were adjusted to  $1 \times 10^6$  cells per 100

µl staining buffer and incubated with PE-anti-EpCAM (eBioscience), FITC-anti-CD45, and APC-anti-IL-22R1 (R&D systems, Minneapolis, MN) antibodies for 30 min at 4°C in the dark. FACS data were obtained from BD Caliber and analyzed by Flowjo software (Tree Star Inc., Ashland, OR).

*Isolation of LPCs from DDC-fed mice by Magnetic Activated Cell Sorting (MACS).* Mice were anaesthetized by intraperitoneal pentobarbital injection. LPCs were isolated by a modification of a two-step perfusion protocol, followed by MACS positive and negative selection. The liver was perfused via the hepatic portal vein with EGTA buffer (0.5mM EGTA, 137mM NaCl, 4.7mM KCl, 1.2mM KH<sub>2</sub>PO<sub>4</sub>, 0.65mM MgSO<sub>4</sub>, 10.07mM HEPES, pH 7.4) at a flow rate of 5 ml/min for 10 min, followed by collagenase buffer (67mM NaCl, 6.7mM KCl, 4.76mM CaCl<sub>2</sub>, 100.7mM HEPES, 0.035% collagenase type I [Sigma-Aldrich], pH 7.6) at a flow rate of 5 ml/min for 11 min. Livers were dissected in Williams' E medium and dissociated by pipetting. The resulting cell suspension was pelleted, transferred to a trypsinising flask containing 0.1% collagenase type VIII (Sigma-Aldrich), 0.09% Pronase (Roche Diagnostics, Chicago, IL), 0.025% trypsin/0.01% EDTA (Invitrogen), 0.004% DNase (Sigma-Aldrich) in PBS and incubated for 50 min at 37°C. After incubation, an equal volume of cold Williams' E medium containing 2% fetal bovine serum (FBS) was added; the cell suspension was filtered through a 40 µm BD Falcon cell strainer (BD Biosciences) and washed three times. LPCs were purified by centrifugation through a discontinuous gradient of 20 and 50% Percoll (Amersham Biosciences, Piscataway, NJ) in PBS at 1400×g for 20 min. Cells in the middle layer were collected for FACS staining or MACS purification.

For MACS purification, liver nonparenchymal cells from the middle layer were labeled with FITC-anti-CD45 antibodies (BD Biosciences) and incubated with anti-FITC magnetic beads (Miltenyi Biotec, Auburn, CA). CD45<sup>-</sup> cells were collected through negative selection, and then incubated with PE-anti-EpCAM (eBioscience, San Diego, CA) and anti-PE magnetic beads (Miltenyi Biotec). EpCAM<sup>+</sup> cells were collected through positive selection for further experiments.

*Culture of mouse LPC cell line BMOL cells:* Mouse BMOL cells, which were kindly provided by Dr. Yeoh, were cultured in Williams' E medium containing 5% FCS, antibiotics, glutamine, 20 ng/ml epidermal growth factor (EGF, BD Biosciences), 30 ng/ml human insulin-like growth factor II (IGF-II, Sigma-Aldrich). For IL-22 treatment experiments, cells were cultured in serum free Williams' E medium overnight, then IL-22 was added to the medium for various time periods. For BrdU incorporation assay in freshly isolated cells, BrdU (10  $\mu$ M) was added to culture medium and cultured for 24 hours before harvest.

*Acridine orange/ethidium bromide (AO/EB) staining.* Cultured BMOL cells were incubated with AO/EB mixture (final concentration 1 $\mu$ g/ml) for 5 min in 37°C and were visualized immediately under a fluorescence microscope.

*ELISA.* Serum IL-22 levels were measured by using an IL-22 ELISA kit (BD Biosciences) according to manufacturer's instruction.

*Western blot.* Western blot was performed as described previously.<sup>3</sup> Protein bands were visualized by an enhanced chemiluminescence reaction (Amersham Biosciences, Piscataway, NJ) or enhanced fluorescence and analyzed on the Typhoon analyzer (GE Healthcare, Piscataway, NJ). Primary antibodies for Bcl2, Bcl-xL and cyclin D were obtained from Cell Signaling Technology.

*Partial hepatectomy model:* Partial hepatectomy surgery was performed as described previously.<sup>4</sup>

*Real-time PCR.* The expression levels of genes were measured by real-time quantitative PCR, using a model ABI7500 real-time PCR detection system (Applied Biosystems, Foster City, CA). Primers used in real-time PCR included: Bcl2: Forward (5'-3') GGTCTTCAGAGACAGCCAGG; Reverse (5'-3') GATCCAGGATAACGGAGGCT. Bcl-xL: Forward (5'-3') GCTGCATTGTTCCCGTAGAG; Reverse (5'-3') GTTGGATGGCCACCTATCTG. Cyclin D: Forward (5'-3')

TCAGGAGCTCCAAAGCAACT; Reverse (5'-3') TTCTTCATCGGGAGCTGGT.

*Administration of IL-22-expressing adenovirus to mice.* IL-22-expressing adenovirus and control vector adenovirus were kindly provided by Drs. M. Zhang and J. Kolls (Louisiana State University, New Orleans, LA) and have previously been described.<sup>3</sup> To amplify adenoviruses, HEK 293 cells were infected with adenovirus expressing IL-22 (Ad-IL-22) or adenovirus-empty vector (Ad-vector) with a multiplicity of infection (MOI) of 1-2. Cells were harvested 2 or 3 days later when the shape of cells became round and were detached from the dish. Adenoviruses were purified from cell lysate by using Adeno-X Maxi Purification Kit (Clonetechn, Mountain View, CA) according to manufacturer's manual. The titration of adenovirus was determined by Adeno-X Rapid Titer Kit (Clonetechn). Mice were injected intravenously with Ad-IL-22 ( $2 \times 10^8$  pfu) or Ad-vector ( $2 \times 10^8$  pfu).

## References:

1. Kofman AV, Morgan G, Kirschenbaum A, Osbeck J, Hussain M, Swenson S, Theise ND. Dose- and time-dependent oval cell reaction in acetaminophen-induced murine liver injury. *Hepatology* 2005;41:1252-61.
2. Kuwahara R, Kofman AV, Landis CS, Swenson ES, Barendsward E, Theise ND. The hepatic stem cell niche: identification by label-retaining cell assay. *Hepatology* 2008;47:1994-2002.
3. Ki SH, Park O, Zheng M, Morales-Ibanez O, Kolls JK, Bataller R, Gao B. Interleukin-22 treatment ameliorates alcoholic liver injury in a murine model of chronic-binge ethanol feeding: role of signal transducer and activator of transcription 3. *Hepatology* 2010;52:1291-300.
4. Wang H, Park O, Lafdil F, Shen K, Horiguchi N, Yin S, Fu XY, Kunos G, Gao B. Interplay of hepatic and myeloid signal transducer and activator of transcription 3 in facilitating liver regeneration via tempering innate immunity. *Hepatology* 2010;51:1354-62.

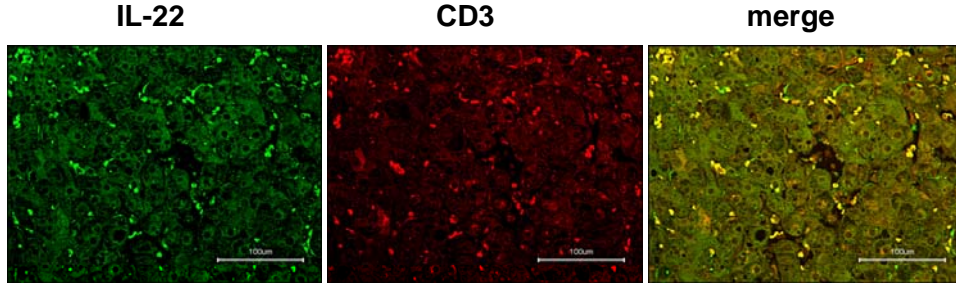
## Supplemental Table 1.

### Characteristics of 64 patients with chronic HBV infection

Gender	Age	Patient No.	Inflamm-atory Grade	Fibrotic Stage	ALT	AST	Number of CK19+ cells	Number of IL-22+ cells	Diagnosis	Sample collection
M	37	1	2	4	17	26	34	51	Compensated cirrhosis	biopsy
M	42	2	1	2	28	34	16	5	Chronic hepatitis B	biopsy
M	45	3	1	2	92	69	19	15	Chronic hepatitis B	biopsy
M	35	4	3	3	45	29	88	68	Chronic hepatitis B	biopsy
M	32	5	3	4	100	63	118	21	Compensated cirrhosis	biopsy
M	51	6	2	2	28	30	83	54	Chronic hepatitis B	biopsy
F	56	7	3	3	55	41	38	6	Chronic hepatitis B	biopsy
F	38	8	2	2	72	59	23	15	Chronic hepatitis B	biopsy
M	51	9	2	2	268	159	20	28	Chronic hepatitis B	biopsy
M	34	10	3	3	43	55	98	24	Chronic hepatitis B	biopsy
M	46	11	3	3	76	47	76	30	Chronic hepatitis B	biopsy
M	38	12	3	4	92	50	105	73	Compensated cirrhosis	biopsy
M	29	13	1	3	57	62	39	5	Chronic hepatitis B	biopsy
F	52	14	3	3	59	55	81	48	Chronic hepatitis B	biopsy
M	47	15	1	2	97	59	18	4	Chronic hepatitis B	biopsy
M	30	16	1	2	82	50	21	5	Chronic hepatitis B	biopsy
M	35	17	3	3	52	29	80	2	Chronic hepatitis B	biopsy
M	34	18	2	2	82	45	32	29	Chronic hepatitis B	biopsy
F	37	19	2	2	19	30	20	30	Chronic hepatitis B	biopsy
M	30	20	1	4	60	40	123	85	Compensated cirrhosis	biopsy
M	36	21	3	3	55	46	63	13	Chronic hepatitis B	biopsy
M	27	22	1	1	72	62	51	13	Chronic hepatitis B	biopsy
M	46	23	3	4	271	171	87	39	Active cirrhosis	biopsy
M	50	24	2	3	49	32	25	13	Chronic hepatitis B	biopsy
M	45	25	3	3	73	67	67	24	Chronic hepatitis B	biopsy
M	46	26	2	2	42	52	70	40	Chronic hepatitis B	biopsy
M	28	27	3	3	22	12	76	42	Chronic hepatitis B	biopsy
M	28	28	2	2	50	25	50	42	Chronic hepatitis B	biopsy
F	30	29	1	2	35	139	43	12	Chronic hepatitis B	biopsy
M	35	30	3	4	124	84	118	48	Compensated cirrhosis	biopsy
M	26	31	3	3	108	145	101	58	Chronic hepatitis B	biopsy
M	25	32	3	3	112		67	67	Chronic hepatitis B	biopsy
M	27	33	2	2	97	82	28	8	Chronic hepatitis B	biopsy
M	21	34	2	2	99	45	25	14	Chronic hepatitis B	biopsy
M	30	35	2	3	66	82	120	7	Chronic hepatitis B	biopsy
F	35	36	1	2	56	62	19	4	Chronic hepatitis B	biopsy
M	39	37	1	1	220	170	2	2	Chronic hepatitis B	biopsy
M	30	38	2	2	78	37	17	4	Chronic hepatitis B	biopsy
M	45	39	2	2	20	17	26	50	Chronic hepatitis B	biopsy
M	29	40	2	2	67	51	23	11	Chronic hepatitis B	biopsy
M	36	41	2	2	61	63	23	57	Chronic hepatitis B	biopsy
M	33	42	2	4	17	34	34	42	Compensated cirrhosis	biopsy

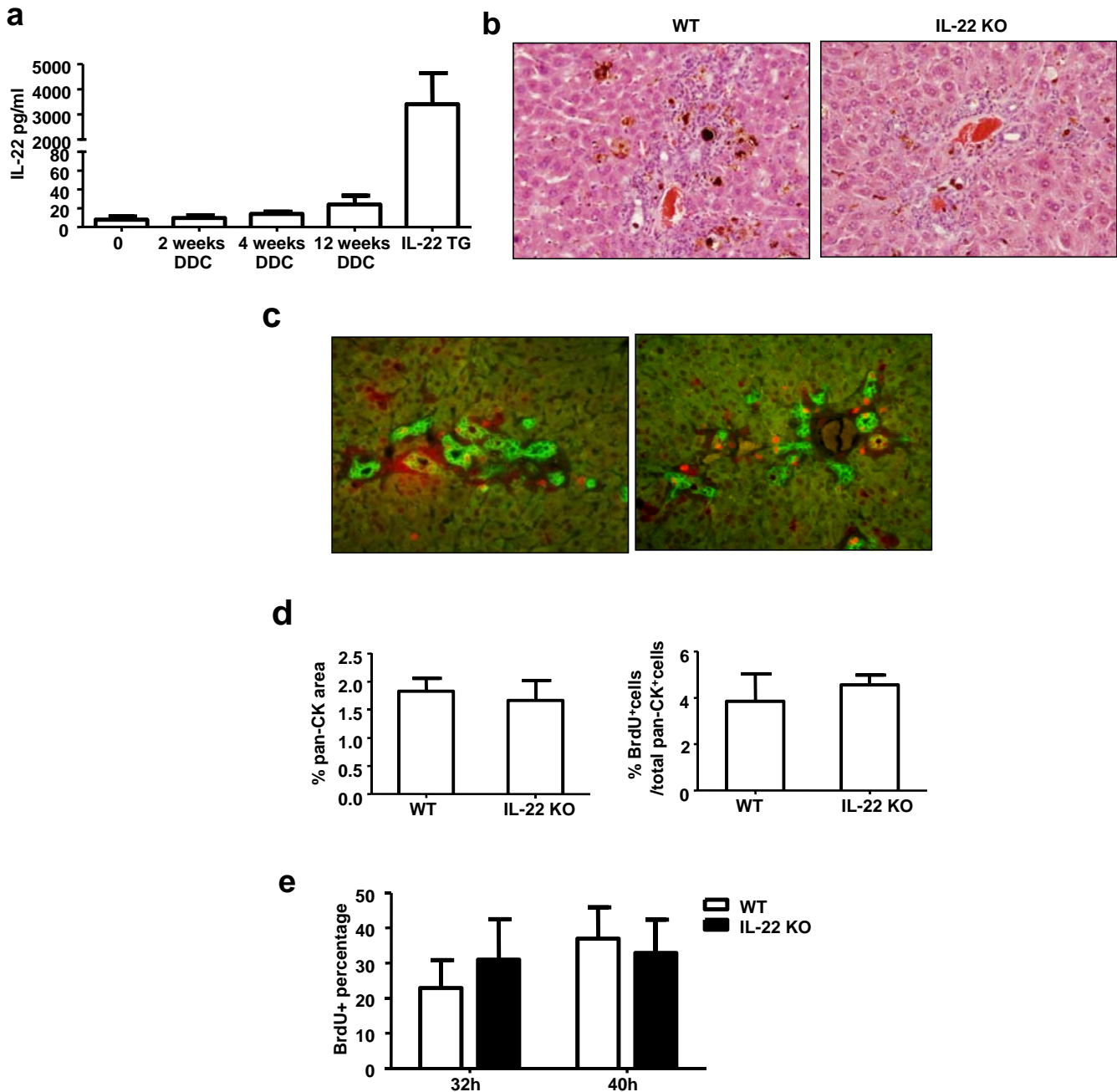
M	35	43	2	2	48	146	23	15	Chronic hepatitis B	biopsy
F	28	44	3	3	145	196	45	29	Chronic hepatitis B	biopsy
M	42	45	1	1	68	90	10	25	Chronic hepatitis B	biopsy
M	37	46	2	3	39	39	48	36	Chronic hepatitis B	biopsy
M	38	47	4	4	683	159	352	281	Acute on chronic liver failure	explant
M	38	48	4	4	93	193	297	225	Acute on chronic liver failure	explant
M	36	49	4	4	206	141	199	254	Acute on chronic liver failure	explant
M	40	50	4	4	454	258	341	226	Acute on chronic liver failure	explant
F	45	51	3	4	21	22	255	192	Chronic liver failure	explant
M	51	52	4	3	143	339	312	224	Acute on chronic liver failure	explant
M	38	53	4	4	29	32	381	316	Acute on chronic liver failure	explant
F	56	54	4	4	63	71	279	8	Acute on chronic liver failure	explant
M	47	55	4	4	32	28	306	212	Chronic liver failure	explant
M	46	56	4	4	24	48	335	211	Chronic liver failure	explant
F	55	57	4	4	13	36	170	258	Chronic liver failure	explant
M	44	58	4	4	170	146	289	253	Acute on chronic liver failure	explant
M	40	59	4	4	60	45	274	181	Chronic liver failure	explant
M	63	60	4	4	20	33	257	232	Chronic liver failure	explant
M	60	61	4	4	79	56	298	199	Acute on chronic liver failure	explant
M	29	62	4	4	31	91	401	327	Chronic liver failure	explant
F	38	63	2	4	44	36	143	50	Compensated cirrhosis	explant
F	39	64	0	4	31	28	151	73	Compensated cirrhosis	explant

## Feng et al.: Supplemental Fig. S1



**Supplemental Fig. S1: CD3<sup>+</sup> T cells are the major source of IL-22 in the livers from HBV patients.** Liver samples from human HBV patients were stained with anti-IL-22 and anti-CD3 antibodies. Most IL-22<sup>+</sup> cells were co-localized with CD3<sup>+</sup> T cells. Representative photographs from 25 HBV-infected livers with similar results are shown.

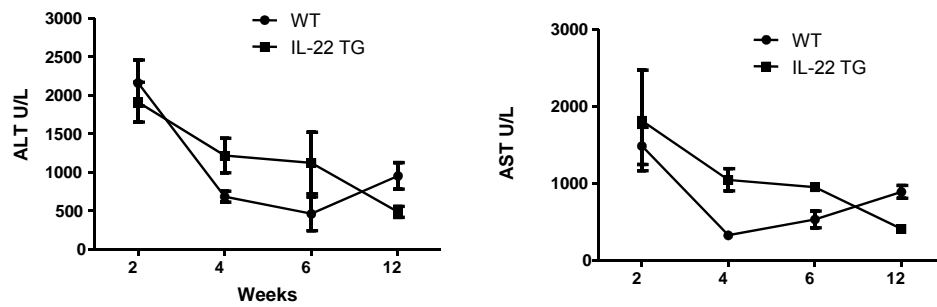
## Feng et al.: Supplemental Fig. S2



**Supplemental Fig. S2: Similar LPC proliferation in WT mice and IL-22 KO mice after DDC diet feeding.** (a) Mice were fed DDC diet for various time points, serum IL-22 levels were measured. (b) H&E staining of liver tissues from 2-week DDC-fed WT and IL-22 KO mice. (c) Pan-CK (green)/BrdU (red) double staining of liver tissues from 2-week DDC fed-WT and IL-22TG mice with BrdU injection 2 h before sacrifice. (d) Quantification of the pan-CK<sup>+</sup> area and BrdU<sup>+</sup>pan-CK<sup>+</sup> double positive cells. (e) Quantification of BrdU<sup>+</sup>hepatocytes in WT mice and IL-22 KO 32 and 40 h after 2/3 partial hepatectomy. Values represent means  $\pm$  SD (n=6=10).

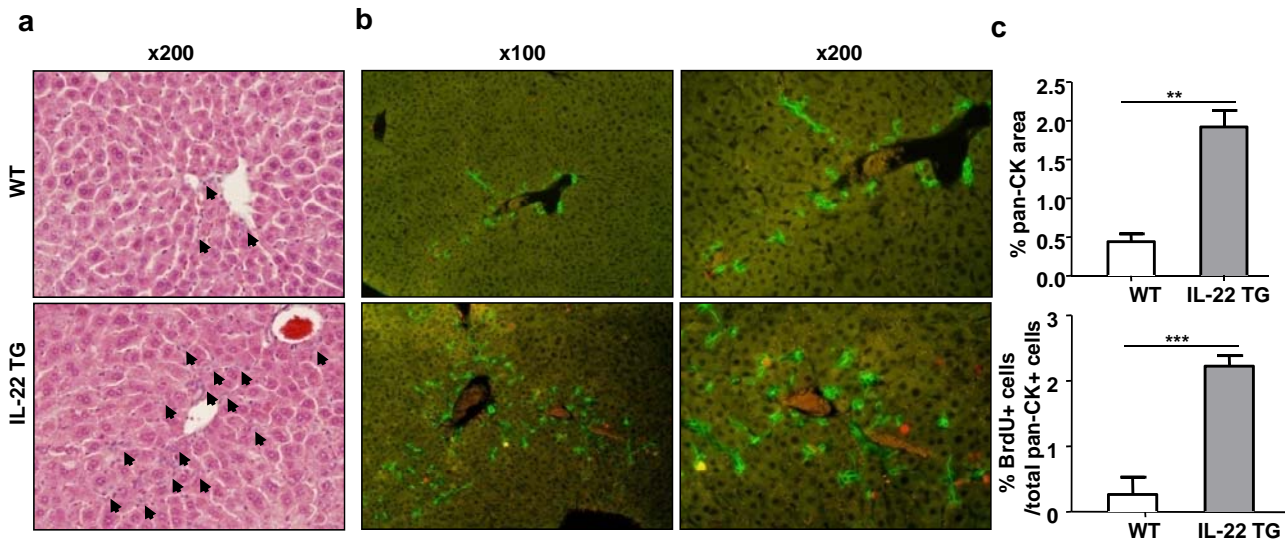


## Feng et al.: Supplemental Fig. S3



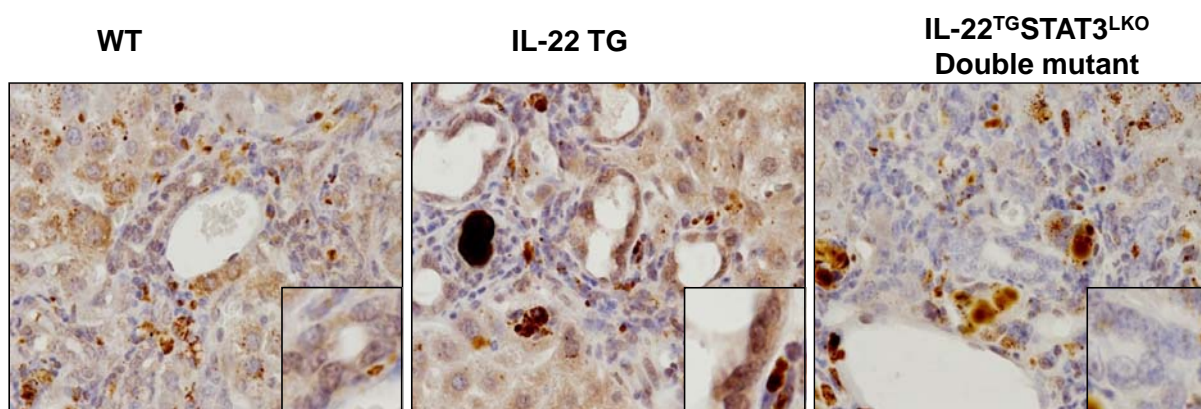
**Supplemental Fig. S3:** WT and IL-22TG mice were fed DDC diet for various time periods. (a) Serum ALT and AST were measured.

## Feng et al.: Supplemental Fig. S4



**Supplemental Fig. S4: Increased LPCs in IL-22TG mice after CDE diet feeding.** Mice were fed CDE diet for 4 weeks. **(a)** H&E staining of liver tissues from CDE-fed WT and IL-22TG mice. **(b)** Pan-CK (green)/BrdU (red) double staining of liver tissues from CDE-fed WT and IL-22TG mice with BrdU injection 2 h before sacrifice. **(c)** Quantification of the pan-CK<sup>+</sup> area and BrdU<sup>+</sup>pan-CK<sup>+</sup> double positive cells. \*\* $P < 0.01$ , \*\*\* $P < 0.001$

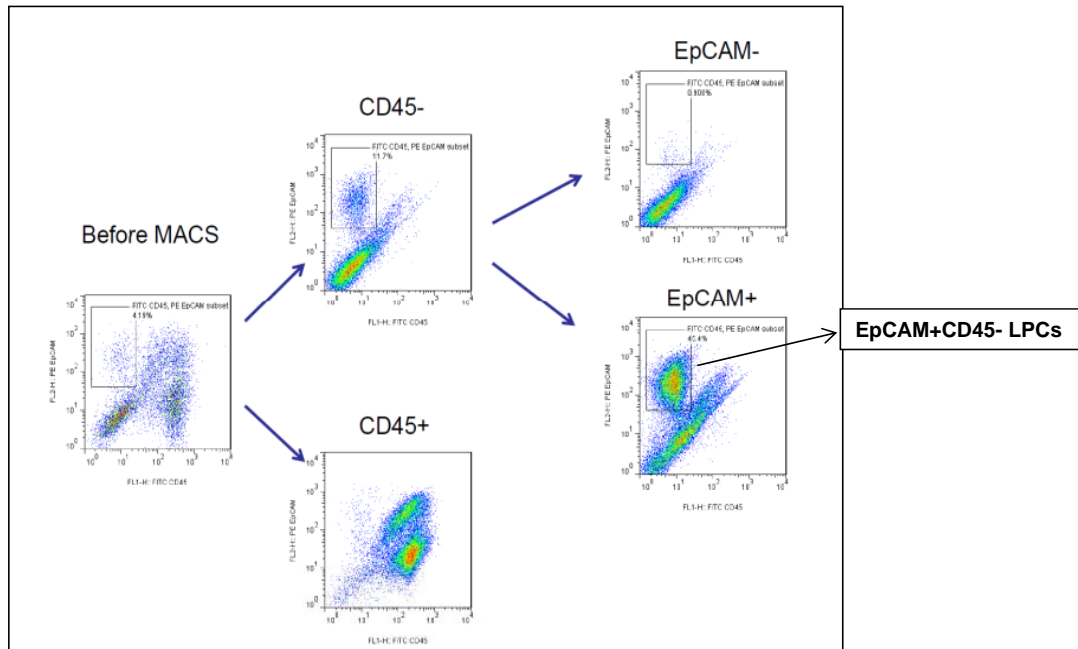
**Feng et al.: Supplemental Fig. S5**



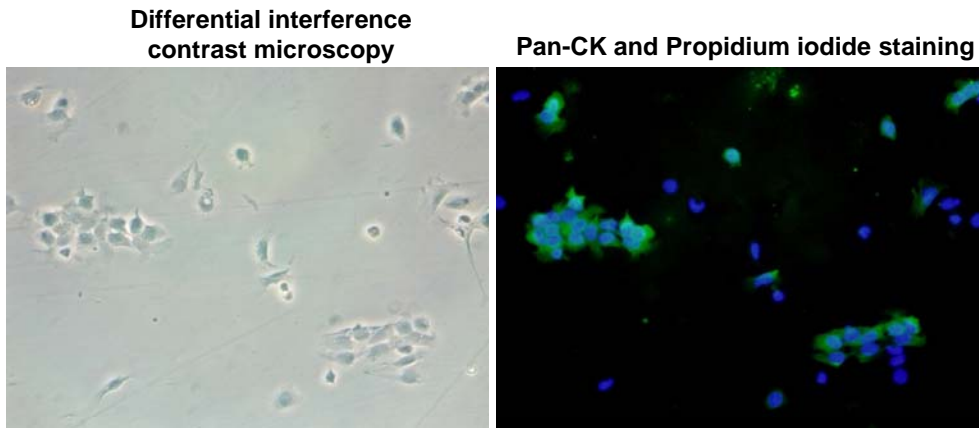
**Supplemental Fig. S5: STAT3 was deleted in LPCs of IL-22<sup>TG</sup>STAT3<sup>LKO</sup> mice.** WT, IL-22TG and IL-22<sup>TG</sup>STAT3<sup>LKO</sup> double mutant mice were fed DDC diet for 4 weeks. Liver sections were stained with anti-STAT3 antibody and visualized by DAB. Brown staining is positive for STAT3 protein.

Feng et al.: Supplemental Fig. S6a-b

a

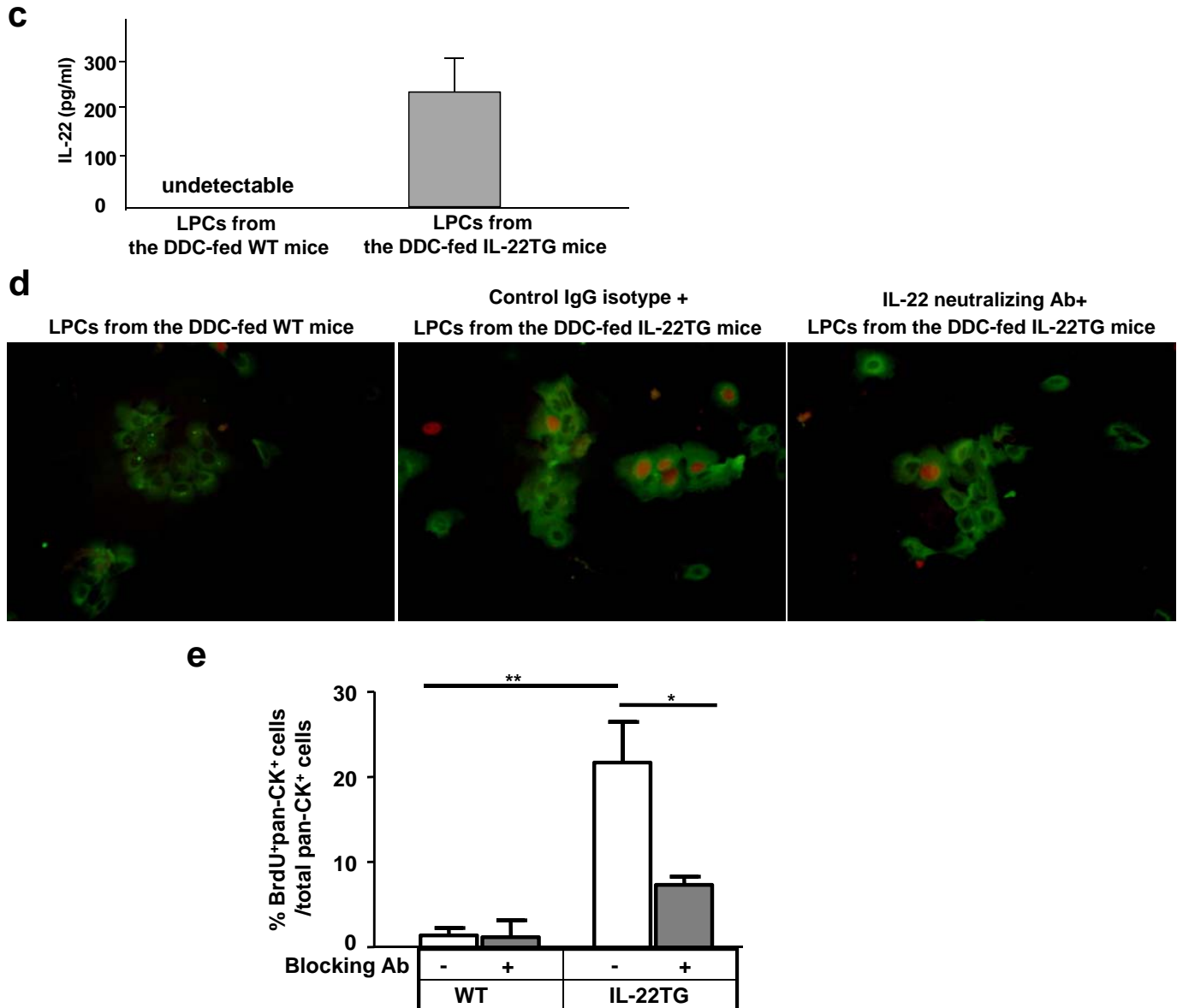


b



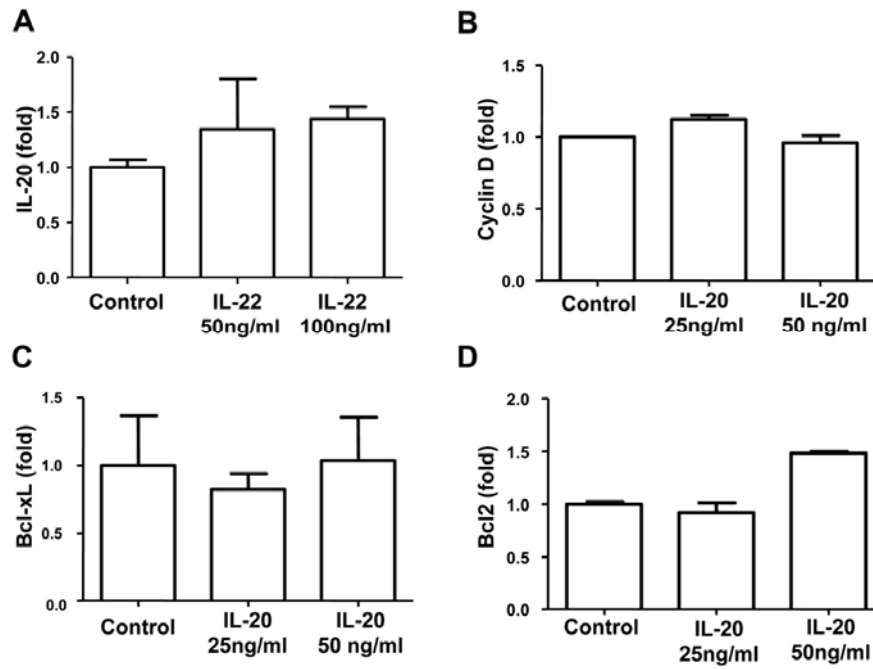
**Supplemental Fig. S6:** (a) LPCs were purified from DDC-fed mice by using two-step MACS purification process. Liver nonparenchymal cells were stained with FITC-anti-CD45 and PE-anti-EpCAM. CD45<sup>+</sup> cells were depleted in the first step and EpCAM<sup>+</sup> cells were positively selected in the second step. (b) Primary LPCs were isolated from DDC-fed mice, cultured *in vitro* and stained with anti-pan-CK antibody. Nuclei were stained with Propidium iodide. About 70-80% purified cells are pan-CK positive.

## Feng et al.: Supplemental Fig. S6c-e



**Supplemental Fig. S6.** LPCs from the DDC-fed IL-22TG mice proliferate faster *in vitro* compared with those from the DDC-fed WT mice, which is suppressed by the treatment with an IL22 neutralizing antibody. WT and IL-22TG mice were fed a DDC diet for 4 weeks. **(c)** LPCs were purified and cultured *in vitro* for 24h, and the supernatants were then collected for the measurement of IL-22 levels. **(d)** Purified LPCs were cultured in serum free medium with or without IL-22 blocking antibody (5µg/ml, from R&D system). BrdU (10 µM) was added to culture medium 24h before harvest. Pan-CK (green) and BrdU (red) double staining were performed to evaluate cell proliferation. **(e)** Quantification of percentage of BrdU<sup>+</sup>pan-CK<sup>+</sup> cells in total pan-CK<sup>+</sup> cells. \*\* $P < 0.01$ , \* $P < 0.05$ .

## Feng et al.: Supplemental Fig. S7



**Supplemental Fig. S7.** IL-22 does not upregulate IL-20 mRNA expression in BMOL cells, and IL-20 does not upregulate expression of cyclin D, Bcl-xL, and Bcl-2 in BMOL cells.